Supplemental Information

Diet-induced alterations in gut microflora contribute to lethal pulmonary damage in TLR2/TLR4 deficient mice

Yewei Ji, Shengyi Sun, Julia K. Goodrich, Hana Kim, Angela C. Poole, Gerald E. Duhamel, Ruth E. Ley, and Ling Qi

Corresponding author: Ling Qi, Ph.D.; lq35@cornell.edu; Phone: (607) 254-8857; FAX: (607) 255-6249

SUPLEMENTAL EXPERIMENTAL PROCEDURES

RNA extraction and quantitative (Q)-PCR. RNA extraction from cells and tissues, and Q-PCR were carried out as previously described (Ji et al., 2012b; Sun et al., 2012) using Trizol (Invitrogen). Q-PCR data collected on the Roche LightCycler 480 were normalized to ribosomal *l32* gene in the corresponding sample. Primer sequences are the following: *Tnfa,* TCAGCCGATTTGCTATCTCATA (Forward), AGTACTTGGGCAGATTGACCTC (Reverse); *Nlrp3,* GTGGTGACCCTCTGTGAGGT (Forward), TCTTCCTGGAGCGCTTCTAA (Reverse); *Mip1a,* TTCTCTGTACCATGACACTCTGC (Forward), CGTGGAATCTTCCGGCTGTAG (Reverse); *Lyz1,* GCCAAGGTCTACAATCGTTGTGAGTTG (Forward), CAGTCAGCCAGCTTGACACCACG (Reverse); *Il6,* AGACAAAGCCAGAGTCCTTCAG (Forward), TGCCGAGTAGATCTCAAAGTGA (Reverse); *Il1b,* CCAAGCAACGACAAAATACC (Forward), GTTGAAGACAAACCGTTTTTCC (Reverse); *Il18,* GCTGTGACCCTCTCTGTGAA (Forward), GGCAAGCAAGAAAGTGTCCT (Reverse); *Ifng,* GCGTCATTGAATCACACCTG (Forward), TGAGCTCATTGAATGCTTGG (Reverse); *Defa21,* CCAGGGGAAGATGACCAGGCTG (Forward), TGCAGCGACGATTTCTACAAAGGC (Reverse); *Defa1,* TCAAGAGGCTGCAAAGGAAGAGAAC (Forward), TGGTCTCCATGTTCAGCGACAGC (Reverse); *Defa-rs1,* CACCACCCAAGCTCCAAATACACAG (Forward), ATCGTGAGGACCAAAAGCAAATGG (Reverse); *Cr2,* CCAGGCTGATCCTATCCAAA (Forward), GTCCCATTCATGCGTTCTCT (Reverse); *Caspase1,* AGATGCCCACTGCTGATAGG (Forward), TTGGCACGATTCTCAGCATA (Reverse); *Asc,* CCAGTGTCCCTGCTCAGAGT (Forward), TCATCTTGTCTTGGCTGGTG (Reverse); *Ocln,* GATGCAGGTCTGCAGGAGTA (Forward), TCCCACCATCCTCTTGATGT (Reverse); *Cdh1,*CCTGCCAATCCTGATGAAAT (Forward), GTCCTGATCCGACTCAGAGG (Reverse); *JAM1,* GGCAGCTGTCCTGGTAACAC (Forward), GGAACGACGAGGTCTGTTTG (Reverse); *Cgn,* GACAGTTCTGCAGTCCACCA (Forward), CCGCTCAATTTCCTCTTCTG (Reverse); *Rantes,* GCTGCTTTGCCTACCTCTCC (Forward), TCGAGTGACAAACACGACTGC (Reverse); *Nlrp1,* CACTGCCCAAGATTGCTACA (Forward), CTTCACTCAGCACCAGACCA (Reverse); *Nfkbia,* CTCCAGATGCTACCCGAGAG (Forward), CATTCTTTTTGCCACTTTCCA (Reverse); *Emr1,* TGCTGTTCAGAACCACAATACC (Forward), CACTGCCTCCACTAGCATCC (Reverse); *Il12a,* CAGCACTTCAGAATCACAACC (Forward), AGCTCAGATAGCCCATCACC (Reverse); *Nos2*, CCAAGCCCTCACCTACTTCC (Forward), CTCTGAGGGCTGACACAAGG (Reverse); *ZO1,* CCCTGAAAGAAGCGATTCAG (Forward), CCCGCCTTCTGTATCTGTGT (Reverse); *Cldn1,* TTAGTGGCCACAGCATGGTA (Forward), GAAGGTGTTGGCTTGGGATA (Reverse); *Bcl2,* AGTACCTGAACCGGCATCTG (Forward), GCTGAGCAGGGTCTTCAGAG (Reverse).

Ileal epithelial cell purification. After fat and connective tissue were removed, ileum was cut longitudinally to expose luminal surface and contents were gently removed. After cut into small pieces and washed with PBS, the intestinal pieces were placed in 5 ml of 30 mM EDTA in PBS, incubated at 37^{o}C on a shaker for 20 min, vortexed for 15 sec at max setting, and allowed to sit on the bench for 5 min. Supernatant were transferred to a new collection tube and centrifuged at 300 x *g* for 10 min at 4^{o}C. Pellets consisted of ileal epithelial cells were snap frozen in liquid nitrogen. The purity of ileal epithelial cells was examined using Q-PCR analysis of the enterocyte-specific gene *villin* and leukocyte-specific gene *Cd45*. And the purified cells were used to test the transcription level of antibacterial peptides and tight junction genes (Fig S5).

Immunohistochemistry. IHC were performed as we recently described (Sun et al., 2014). Briefly, **p**araffin-embedded intestinal sections were rehydrated, boiled in 1mM EDTA for antigen retrieval, and stained with Histostain kit, DAB substrate (Invitrogen) or fluorescence-conjugated secondary antibody. Primary antibodies used for IHC were: PCNA (rabbit, 1:100) and Lysozyme

C (goat, 1:200) from Santa Cruz. H&E and IHC slides (for PCNA) were scanned using the Aperio Scanscope and pictures were taken at indicated magnifications. Fluorescence Images were captured under a Zeiss LSM710 confocal microscope at Cornell Biotechnology Resource Center Imaging Facility.

Staining for Gram positive and negative bacteria. Staining was performed by the Histology Core Laboratory at Cornell on a fee for service basis. Briefly, the section was deparaffinized, hydrated in distilled water, soaked in Hucker-Conn solution for 3 min followed by Langeron's iodine for 3 min. After washes in deionized water for 1 min, slides were dipped quickly 1-4 times in acetone until no more blue dye was visibly released. Slides were then satined with fast Green-Safranin working solution for 3 min, and rinsed in 100% ETOH. Slides were differentiated with few dips in 1% alcoholic acetic acid until no more dye was visibly released. Finally, slides were rinsed briefly in 100% ETOH, cleared in xylene and mounted with mounting medium.

TUNEL staining. TUNEL staining were performed as we recently described (Sun et al., 2014). Briefly, paraffin-embedded lung sections were rehydrated, treated with protease K, and stained for 1 hour at 37˚C using the in Situ Death Detection TUNEL Kit (Roche 11684795910). Images were captured under a Zeiss LSM710 confocal microscope at the Cornell Biotechnology Resource Center Imaging Facility.

Flow cytometry. Flow cytometric analysis of immune cells was performed as we previously described (Ji et al., 2012a; Ji et al., 2012b; Xia et al., 2011). Fluorochrome- or biotin-conjugated antibodies against CD3 (145-2C11), TCRβ (H57-597), CD4 (GK1.5), CD8 (YTS169), Gr-1 (RB6-8C5), CD11b (M1/70), CD45 (30-F11), IFN-γ (XMG1.2), TNF-α (MP6-XT22), avidin-PerCP and isotype control antibodies were purchased from BioLegend or BD Biosciences. Data were analyzed using the CellQuest software (BD Biosciences) and Flowjo (Flowjo.com). For intracellular staining of TNF-α and IFN-γ, cells were purified and incubated with 50 ng/ml PMA (Sigma) and monensin (the GolgiStop kit, BD Biosciences) for 3h *in vitro*, and the rest of steps were performed per the Cytofix/Cytoperm^{TM} plus kit protocol (BD Biosciences).

Dextran-FITC uptake. To directly test epithelial permeability and integrity of the intestines, WT and DKO mice were deprived of food and water for 4 hours and then gavaged with non-digestible 4 kDa FITC-dextran (Sigma) at a dose of 0.6 mg/g body weight. 50 µl serum were collected from tail vein at various time points and serum intensity of FITC was measured using the Synergy plate reader (Biotek) with the excitation at 488 nm. Data were plotted against the standard curve of serial dilutions of FITC-dextran.

Serum endotoxin test. Blood were collected from tail vein. 10 µl serum was diluted in 40 µl endotoxin-free water and inactivated at 70˚C for 10 minutes. The endotoxin level was measured using the Limulus Amebocyte Lysate assay kit (QCL-1000^{TM}, Lonza) per its protocol.

References:

Ji, Y., Sun, S., Xia, S., Yang, L., Li, X., and Qi, L. (2012a). Short Term High Fat Diet Challenge Promotes Alternative Macrophage Polarization in Adipose Tissue via Natural Killer T Cells and Interleukin-4. J Biol Chem 287, 24378-24386.

Ji, Y., Sun, S., Xu, A., Bhargava, P., Yang, L., Lam, K.S., Gao, B., Lee, C.H., Kersten, S., and Qi, L. (2012b). Activation of Natural Killer T Cells Promotes M2 Macrophage Polarization in Adipose Tissue and Improves Systemic Glucose Tolerance via Interleukin-4 (IL-4)/STAT6 Protein Signaling Axis in Obesity. J Biol Chem 287, 13561-13571.

Sun, S., Shi, G., Han, X., Francisco, A.B., Ji, Y., Mendonca, N., Liu, X., Locasale, J.W., Simpson, K.W., Duhamel, G.E., Kersten, S., Yates, J.R., 3rd, Long, Q., and Qi, L. (2014). Sel1L is indispensable for mammalian endoplasmic reticulum-associated degradation, endoplasmic reticulum homeostasis, and survival. Proc Natl Acad Sci U S A 111, E582-591.

Sun, S., Xia, S., Ji, Y., Kersten, S., and Qi, L. (2012). The ATP-P2X7 Signaling Axis Is Dispensable for Obesity-Associated Inflammasome Activation in Adipose Tissue. Diabetes 61, 1471-1478.

Xia, S., Sha, H., Yang, L., Ji, Y., Ostrand-Rosenberg, S., and Qi, L. (2011). Gr-1+ CD11b+ Myeloid-derived Suppressor Cells Suppress Inflammation and Promote Insulin Sensitivity in Obesity. J Biol Chem 286, 23591-23599.

Table S1. Comparison of fecal microbiota composition between WT and DKO mice on a HFD for 17 weeks. The complete list of hits identified by Illumina sequencing is shown at the levels of order, genus and OTU. P values were determined by Student's t-test. Blue shaded areas, $P<0.05$.

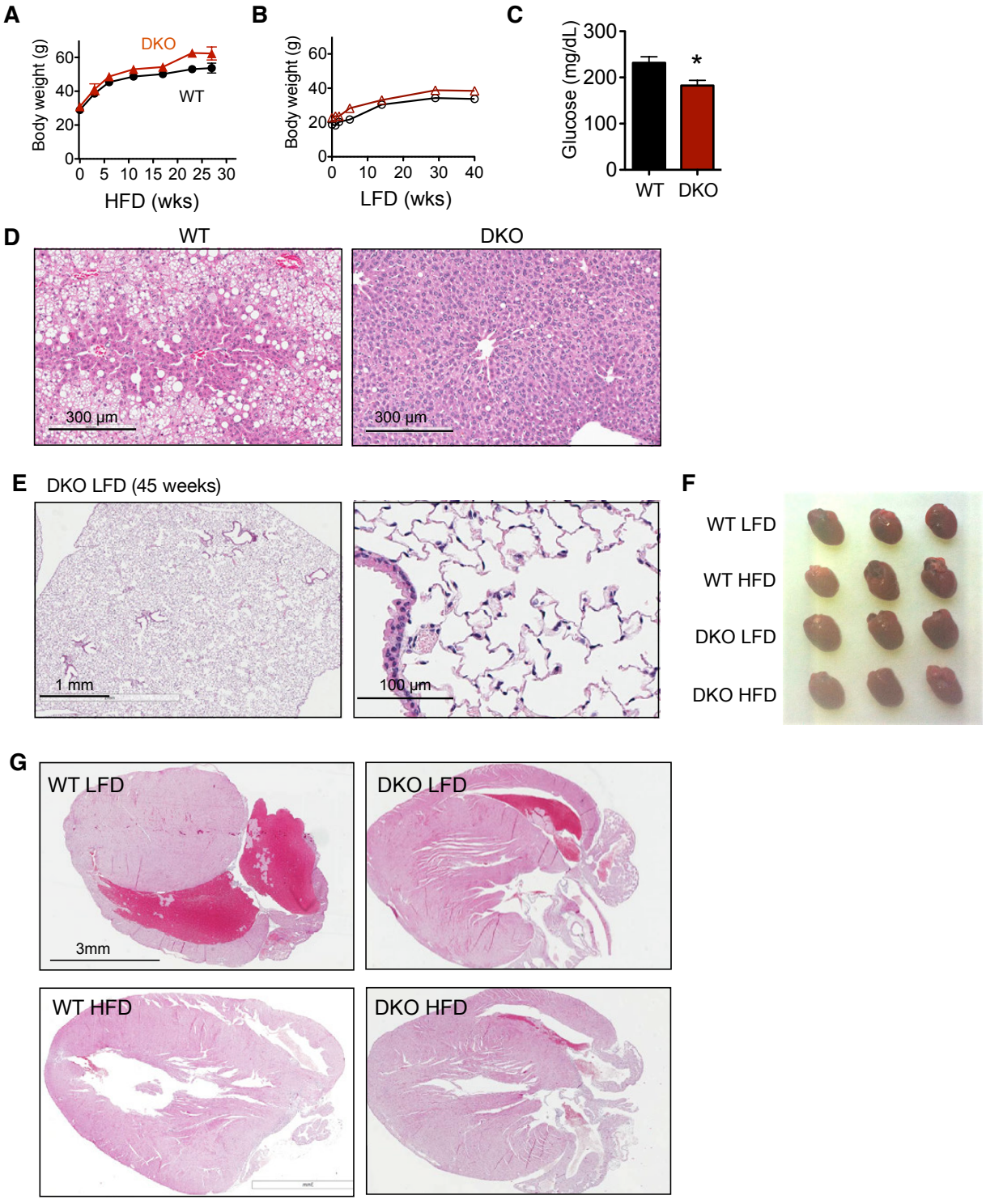

Figure S1. Growth curve, metabolic parameters and non-cardiogenic pulmonary damage in DKO mice on HFD.

(A-B) Growth curves of WT and DKO mice on HFD (A) and LFD (B). N=5-9.
(C) Blood glucose of WT and DKO mice on HFD for 16 weeks following a 6 hour fast. N=5.
(D) Representative H&E images of livers from DKO mice on HFD for 29 weeks. N=3.
(E) Representative H&E images of lungs from DKO mice on LFD for 45 weeks. N=3.
(F-G) Normal heart morphology (F) and H&E images (G) of WT and DKO mice on LFD or HFD for 35 weeks.
*, $p<0.05$, by Student's t test.

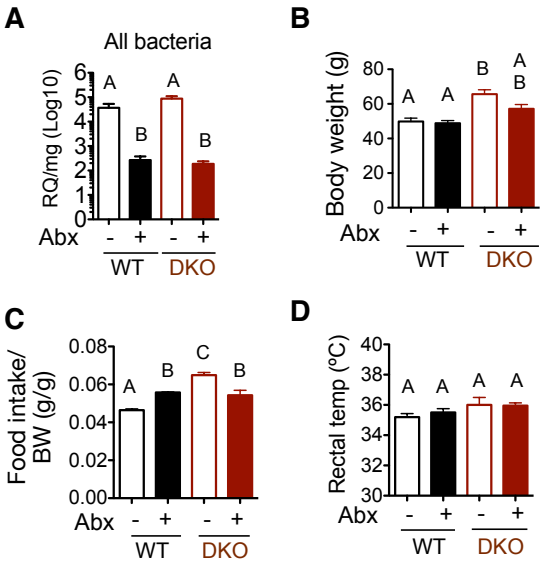

Figure S2. Changes in metabolic parameters following antibiotics treatment.

Fecal bacterial level (A), body weight (B), food intake (C), and rectal temperature (D) of WT and DKO mice fed a HFD with or without antibiotic treatment (Abx). A, 2-week Abx; B-D, 18-21-week Abx. Q-PCR analysis was performed with universal primers of 16S rRNA in fecal DNA samples. Relative quantity (RQ) was generated by normalizing Ct values to universal 16S standard and then to fecal weight (mg). N=3-5.

Values, mean ± s.e.m. Statistical analyses were performed with one-way ANOVA with the Tukey Post-tests (different letters mark statistic significance, i.e. $p < 0.05$).

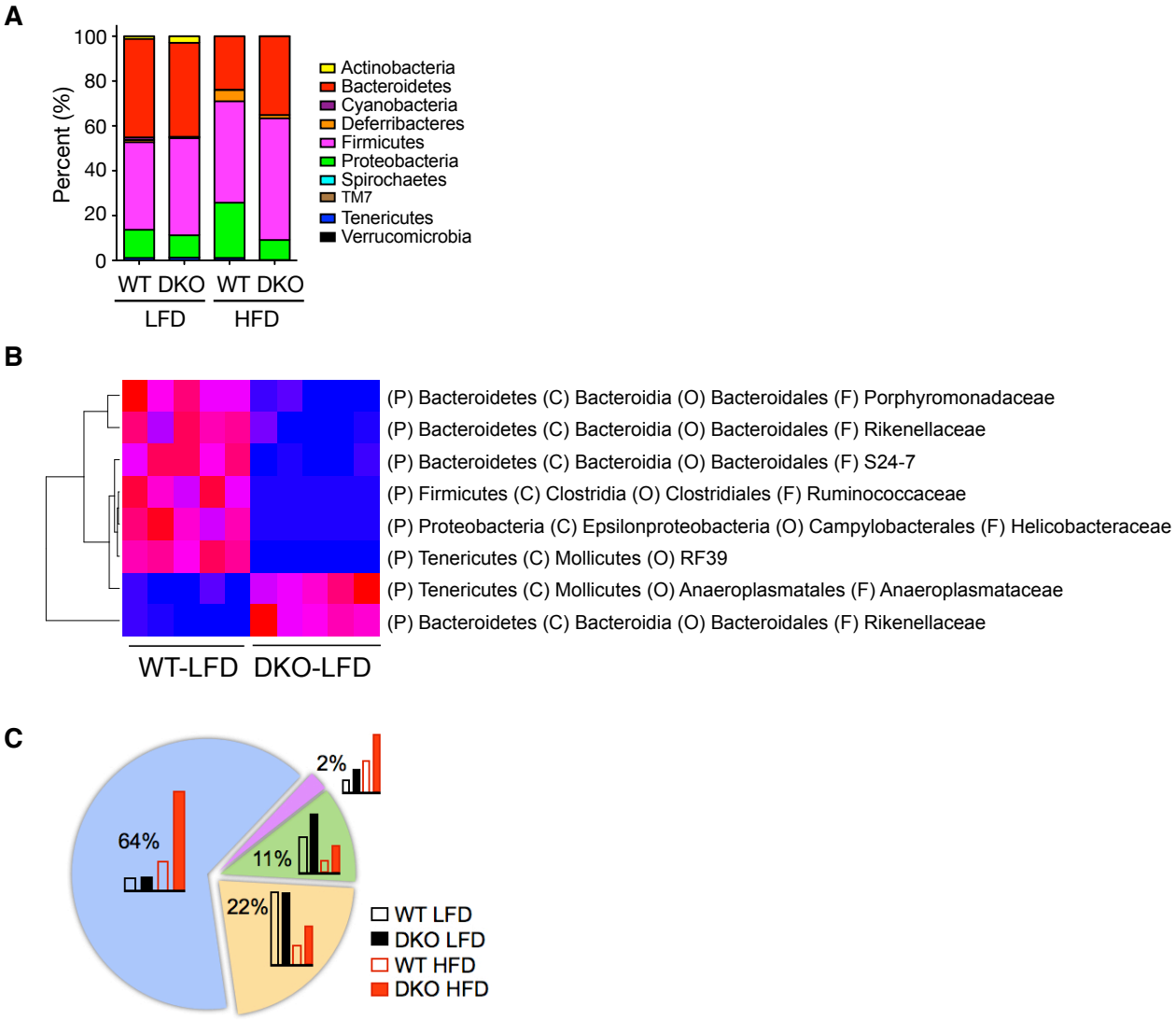

Figure S3. Effect of diet and innate deficiency on fecal bacterial composition.

(A) The relative abundance of fecal microbiota on phylum level in single-housed WT and DKO mice on LFD or HFD for 17 weeks.
(B) Heat map showing the relative abundance of the top bacterial OTUs representing the difference between LFD-fed WT and DKO mice. The phylum (P), class (C), order (O), family (F) of each OTU are indicated.
(C) Pie graph showing 4 categories of changes seen in 87 OTUs that were found higher in DKO mice on HFD vs. WT cohorts on HFD. The percent of each category shown with bars indicating relative pattern among the cohorts. Of note, 56 OTUs (64%) were induced synergistically in DKO HFD mice, pointing to a combined effect of HFD and innate deficiency.

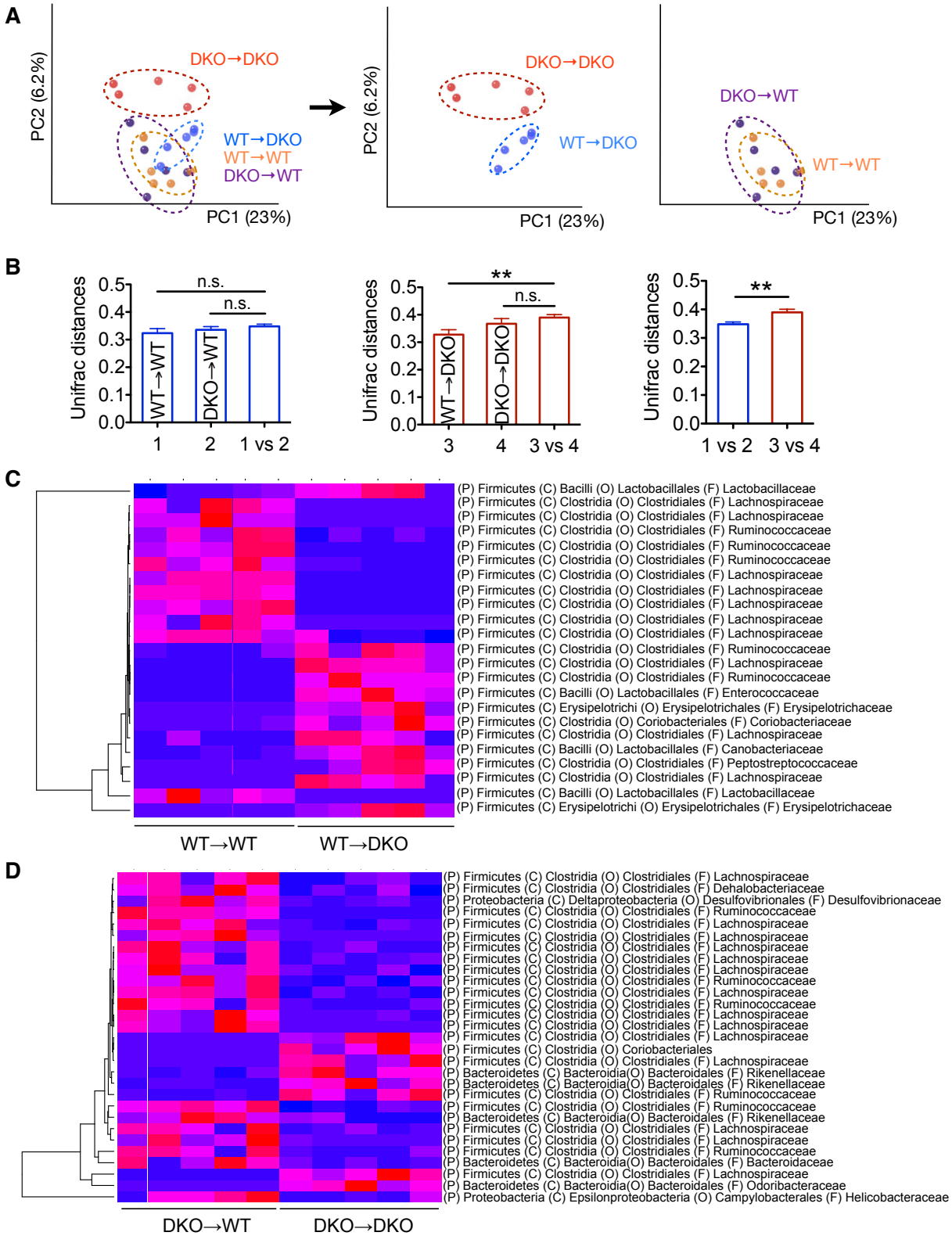

Figure S4. The effect of innate immunity deficiency on microbiota composition.

(A) PCoA analysis of fecal microbiota from single-housed BMT chimeric mice (WT→WT, DKO→WT, WT→DKO and DKO→DKO) fed a HFD for 6 weeks. Note the difference between DKO→DKO and WT→DKO.

(B) The UniFrac distances either within the same BMT group or between two BMT groups. A higher UniFrac distance denotes greater dissimilarity between two mice. **, $p<0.01$ by Student's t test, denoting statistically significant differences between the two sets of UniFrac distances.

(C-D) Heat map showing the relative abundance of the top bacteria OTUs representing the difference between WT→WT and WT→DKO (B) or DKO→WT and DKO→DKO (C) fed a HFD for 6 weeks. Cohorts were age- and gender matched. The phylum (P), class (C), order (O), family (F) of each OTU are indicated.

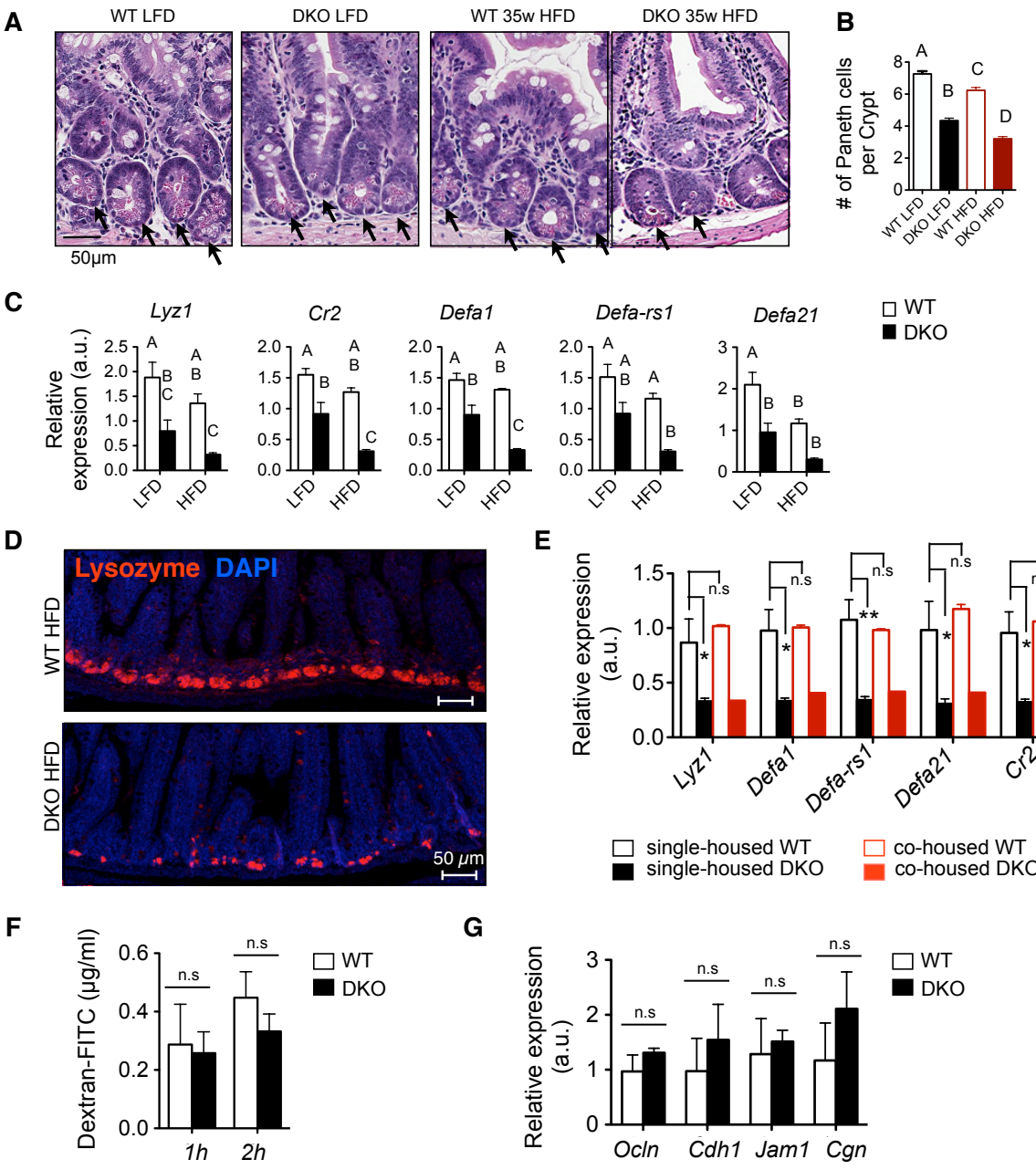

Figure S5. Impaired Paneth cell function in DKO mice on HFD.

(A) Representative H&E images of ileal crypts and Paneth cells in mice fed a LFD or HFD for 35 weeks. Arrows point to the base of the crypts. n=3 mice each.

(B) Quantitation of Paneth cell number in the ileum of mice fed a LFD or HFD for 35 weeks. n= 90-120 crypts from 3 mice each.

(C) Q-PCR analysis of anti-bacterial peptide genes in ileal mucosa of mice on LFD or HFD for 35 weeks. *Lyz1,* lysozyme 1; *Cr2,* defensin alpha 2; *Defa1,* defensin alpha 1; *Defa-rs1,* defensin alpha related sequence 1; *Defa21,* defensin alpha 21. n=3 mice each. (B-C) Statistical analyses were performed with one-way ANOVA with the Tukey Post-tests (different letters mark $p < 0.05$).

(D) Confocal images of Lysozyme C staining in the ileum of mice on HFD for 29 weeks. n=3 mice each.

(E) Q-PCR analysis of anti-bacterial peptide genes in ileal mucosa of mice on HFD for 35 weeks, either single- or co-housed. n=2-3 mice each.

(F) Serum levels of dextran-FITC 1 and 2 hr post-gavage in mice on HFD for 27 weeks. n=5 mice each.

(G) Q-PCR analysis of epithelial tight junction genes in ileal mucosa of WT and DKO mice on HFD for 35 weeks. *Ocln,* occludin; *Cdh1,* cadherin 1; *Jam1,* F11 receptor; *Cgn,* cingulin. n=3 mice each. Q-PCR data are normalized to ribosomal gene *l32.* For panels E, F and G, values, mean ± s.e.m. a.u, arbitrary units. (E-G) *, $p<0.05$;**, $p<0.001$; n.s, not significant by Student's t test.

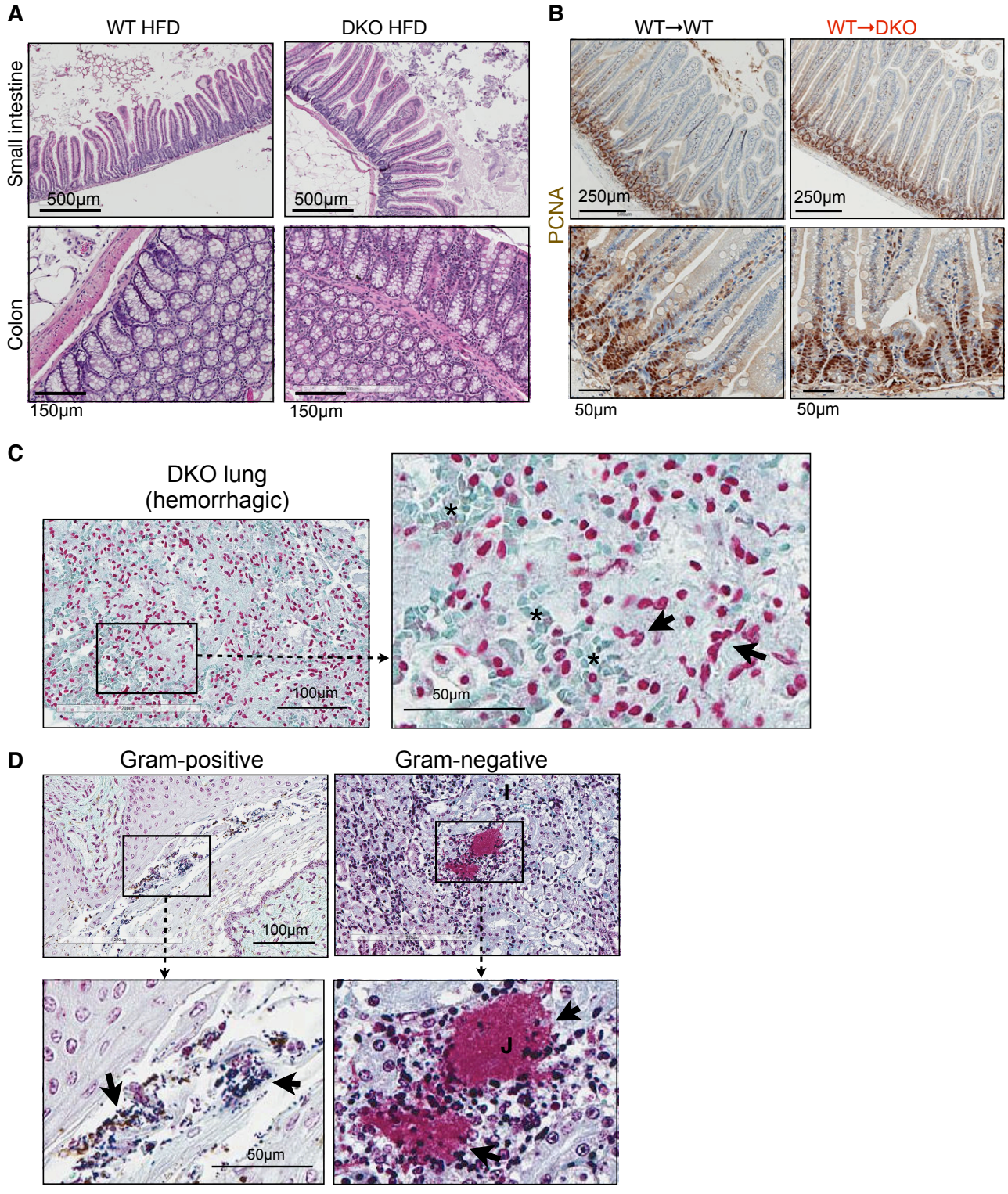

Figure S6. Normal intestinal morphology, epithelial cell proliferation and failure to detect bacteria in the lung of DKO mice on HFD.

(A) Representative H&E images of small intestine and colon morphology in mice fed a HFD for 29 weeks. N=3.
(B) Representative images of PCNA staining (brown) of small intestines of BMT chimeric mice fed a HFD for 17 weeks. N=3.
(C) Representative images of Gram staining of lungs from a DKO mouse that died from severe acute pulmonary damage. No bacteria were detected in the lung. *, red blood cells; arrows, nuclei.
(D) Controls for Gram staining. Left, bovine stomach tissue with gram-positive bacteria stained in blue (arrows). Right, calf kidney tissue with gram-negative bacteria stained in red (arrows).